

# Blending PP with PA6 Industrial Wastes: Effect of the Composition and the Compatibilization

Mohamed Jaziri,<sup>1</sup> Najoua Barhoumi,<sup>2</sup> Valérie Massardier,<sup>3</sup> Flavien Mélis<sup>4</sup>

<sup>1</sup>Unité de Rhéologie, Ecole Nationale des Ingénieurs de Sfax, Rte Soukra 3038 Sfax, Tunisie

<sup>2</sup>Laboratoire de Radio Analyse et Environnement (LRAE), Ecole Nationale des Ingénieurs de Sfax, Rte Soukra 3038 Sfax, Tunisie

<sup>3</sup>Laboratoire des Matériaux Macromoléculaires, Institut National des Sciences Appliquées de Lyon, Unité Mixte de Recherche Centre National de la Recherche Scientifique (INSA Lyon)-UMR/CNRS 5627, 69621 Villeurbanne Cedex, France

<sup>4</sup>Laboratoire des Matériaux Polymères et Biomatériaux, Lyon-Unité Mixte de Recherche UMR/CNRS 5627, 69621 Villeurbanne Cedex, France

Received 25 April 2007; accepted 4 September 2007

DOI 10.1002/app.27542

Published online 3 December 2007 in Wiley InterScience (www.interscience.wiley.com).

**ABSTRACT:** Blending polypropylene to recycled PA6 industrial wastes at different compositions, with and without compatibilizer PPgMA was produced in a corotating twin screw extruder where, polypropylene acts as the polymer matrix and polyamide as the dispersed phase. Several techniques were used to investigate the morphology, thermal, viscoelastic and tensile properties of these blend. Binary PP/PA6 blends showed the presence of PA6 particles dispersed in the PP continuous phase and exhibited a coarse morphology. Increasing PA6 contents in the blend increased their crystallinity and their size and improved the tensile properties at weak deformation. In addition to compatibilizer PPgMA, the morphology shows lower diameters

and a decrease in size of the dispersed PA6 particles. The interfacial adhesion was also improved, as a result of the creation of an interphase that was formed by the interaction between the formed PPgPA6 copolymer in situ and both phases. This interphase induced an improvement in tensile properties. The PPgPA6 copolymer generated by the interphase was identified with DMA analysis thanks to an additional transition in loss modulus curves. © 2007 Wiley Periodicals, Inc. *J Appl Polym Sci* 107: 3451–3458, 2008

**Key words:** recycling; PP/PA6 blend; compatibilization; PPgMA; morphology; thermal; viscoelastic; tensile properties

## INTRODUCTION

There is not only much focus on the recycling of postconsumer solid waste,<sup>1</sup> but also on plastics industry, which has recognized the need of recycling industrial waste to decrease their impact on environment.<sup>1</sup> In fact, all processing techniques produce some residue such as trims of molded parts. Part of this industrial waste consists on engineering resins such as polyamides. Blending polymers represents one of the most attractive routes for polymers recycling.<sup>1</sup> Moreover, mechanical recycling of the industrial polyamide waste is relatively simple<sup>2</sup> and can be used by melt blending with other polymers like polypropylene.

Blending of PA6 with polypropylene combines the thermomechanical properties of polyamide with the insensitivity to humid environments and easy processing characteristics of polypropylene.<sup>1</sup> The well known immiscibility of these systems<sup>3–5</sup> provides the

attractive opportunity of modifying the interaction level to the interface between the components with interface agents. A variety of compatibilizers has been used in PP/PA blends in an attempting to reduce interfacial tension between blend components, suppresses the dispersed phase coalescence, and improves the mechanical properties effectively.<sup>4</sup>

Used compatibilizers are frequently PPgMA (polypropylene grafted with maleic anhydride),<sup>3–8</sup> SEBSgMA (block copolymer polystyrene poly(ethylene-*co*-butyl-1-ene)-polystyrene grafted with maleic anhydride).<sup>9,10</sup> The compatibilizer commonly used at industrial level is PP grafted with maleic anhydride.<sup>11</sup>

Ide and Hasegawa<sup>7</sup> studied the effect of maleic anhydride grafted polypropylene (PPgMA) on PP/PA6 polymer blends. The structural stability and morphology of the blends were greatly improved by PP-g-PA6 grafted copolymers, which were formed by the in situ reaction of anhydride groups with the amino end groups of PA6 during reactive extrusion forming an imidic linkage. Vocke and coworkers<sup>12</sup> have studied analogous systems, using oxazoline-grafted polyolefins or grafted SEBS as an effective compatibilizer in blending polyolefins with engineer-

Correspondence to: M. Jaziri (mohamedjaziri2003@yahoo.fr).

ing plastics. Sacchi et al.<sup>1</sup> reported that compounds PP/PA/PPgMA prepared with recycled PA66 fibres showed flexural modulus higher than compatibilized blends with pristine PA66 and SEM images indicate that the compatibilizer PPgMA is very effective to induce dispersion of recycled PA66 into PP promoting interfacial adhesion.

There are numerous studies<sup>1–12</sup> in literature about the blend of both virgin the PP and PA and the influence of the compatibilization on the morphology, the thermal and mechanical properties, but very few papers<sup>1</sup> have reported the blend of polypropylene with a recycled polyamide using the dynamic-mechanical analyses to study the effect of the compatibilization. Thus, the purpose of this work was to study the mechanical recycled of polyamide industrial waste with blending polypropylene. Blending polypropylene matrix and recycled PA6 as dispersed phase were prepared with and without compatibilizer (PPgMA). Morphological, thermal, dynamic-mechanical, and mechanical analyses were carried out.

## EXPERIMENTAL

### Materials

The polypropylene used in this study was a commercial grade (PP) supplied by Arkema (PPH 7060, MFI = 12 g/10 min at 230°C under 2.16 kg); Recycled material from PA6 industrial waste was supplied by INOPLAST Tunisia. This material was used in the manufacture of the protector of shell oil, which is used in cars. Polypropylene grafted-maleic anhydride (PPgMA) was supplied by Montell products (Qestron KA805), containing 0.9% by weight of maleic anhydride (MA), 0.7% of which by weight is effectively grafted.

### Blend preparation

Prior to blending, the parts of PA6 were crushed and dried at 100°C, in vacuum for 24 h to remove most of absorbed humidity and then identified with FTIR. The extrusion process is carried out in a LEIS-TRITZ twin-screw extruder ( $L/D = 34.5$ ,  $D = 34$  mm) with a screw rotation speed of 150 rpm and a throughput of 3 kg/h. The extrusion zone temperature ranged from 180–245°C.

PP/PA6 blends without compatibilizer were prepared with the following weight composition: (95/5, 90/10, 85/15, and 80/20); compatibilized blends with PPgMA, were prepared to study the compositions PP/PA/Compatibilizer 93.3/5/1.7, 86.7/10/3.3, 85/15/5, and 73.3/20/6.7 (ratio dispersed phase/compatibilizer = 3).

The extrudates were cooled in water and pelletized. Later they are dried under vacuum 24 h at

100°C and then injection molded into standard bars tensile and rectangular bars for DMA analysis, by an injection molding machine (Battenfeld Unilog B2; 350 Plus). The temperatures of the barrel and the mould were maintained at 240 and 60°C, respectively.

### Characterization

#### Morphology analysis

Morphology of the blends was investigated by using a Scanning Electron Microscope (SEM Philips XL 30). The samples were fractured at liquid nitrogen temperature. The fracture surfaces were perpendicular to the mold filling direction of the injection-molded bars and were observed after a gold coating under an accelerating voltage of 30 kV.

#### Thermal properties

Differential Scanning Calorimetry DSC analyses were performed under argon using TA Instruments DSC 2920. Temperature calibration was performed using indium. The specimens (10–20 mg) were placed in sealed aluminium cups, and then cyclically heated from 25 to 250°C at 10°C/min, Equilibrium at 250°C for 1 min, cooled from 250 to 25°C at 10°C/min, Equilibrium at 25°C for 1 min and second heating from 25 to 250°C at 10°C/min. The heats of melting of the samples were measured in the second heating in order to delete the thermal and mechanical history. Crystallinity levels were determined using  $\Delta H_m = 209$  and  $230 \text{ J g}^{-1}$  for hypothetically fully crystalline (100%) PP<sup>13</sup> and PA6.<sup>14</sup>

#### Dynamic mechanical properties

Dynamic-mechanical analysis is a very important tool to show the miscibility between phases in the blend. This analysis was performed under nitrogen atmosphere using DMA, (TA Instruments model 2980) at a heating rate of 3°C/min; the dynamic spectra of  $E''$  were obtained in dual cantilever mode at a vibration frequency of 1 Hz at a temperature from –100 to 120°C under a slight pressure (6 N) with an amplitude of 30  $\mu\text{m}$ . The specimens ( $35 \times 9.7 \times 4 \text{ mm}^3$ ) were injection molded on the Battenfeld molder.

#### Tensile properties

Tensile tests were performed on LLYOD LR 5 KN machine at room temperature using bars specimens (HALTERE H2). Crosshead speed was 5 mm/min. All the reported results for tensile determination are the average of at least 5 measurements.

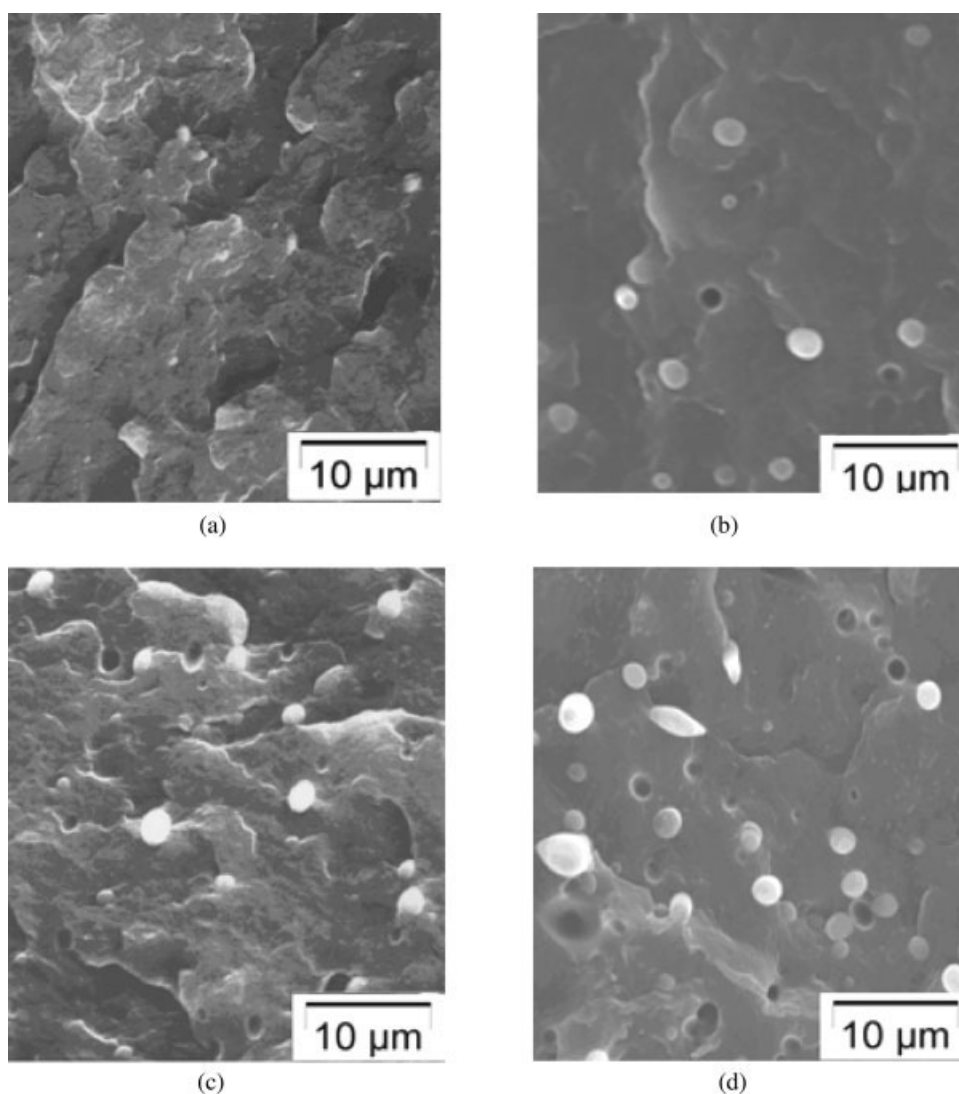


**Figure 1** SEM micrographs of the uncompatibilized blends: (a) PP/PA6 (95/5), (b) PP/PA6 (90/10), (c) PP/PA6 (85/15), (d) PP/PA6 (80/20).

## RESULTS AND DISCUSSION

### SEM Morphologies

Figure 1(a–c) shows SEM micrographs of PP/PA6 blend with 5, 10, 15, and 20 wt % PA6, respectively. The uncompatibilized blends of all compositions tested [Fig. 1(a–c)] showed visual evidence of the incompatibility between PP and PA6, it can be seen that PA6 is dispersed as spherical particles in a continuous PP matrix and show a large distribution of sizes for example from 0.45 to 5  $\mu\text{m}$  in the composition 20 wt % PA6 [Fig. 1(c)]. The dispersed phase is unstable due to the coalescence of spheres during melt processing and consequently forms a coarse morphology.<sup>15</sup> There is also evidence of poor interfacial bonding in this system, with particles of PA6 pulled from the PP matrix lying loose on the fracture surface and with some microvoids observed around

PA6 nodules. The size of the dispersed PA6 particles increases with the PA6 content and the distribution is broad; there is no evidence in adhesion between the two phases. This behaviour agrees with the studies of Wilkinson et al.<sup>15</sup> and Sacchii et al.<sup>1</sup>

With the addition of the compatibilizer PP-g-MA (Fig. 2), the particles of the dispersed phase in the compatibilized blend, in comparison with the uncompatibilized blend, seem to be firmly embedded in the matrix and the dispersed phase boundaries become unclear, as shown in Figure 2(a,b). In Figure 2b, the dispersed phase became more uniform and much reduced in size, the dispersed particles were smaller than 1  $\mu\text{m}$ . The structural stability and morphology of the blends were improved greatly by PP-g-PA6 grafted copolymers that were formed by the in situ reaction of anhydride groups with the amino end groups of PA6.<sup>7</sup> This result indicates the

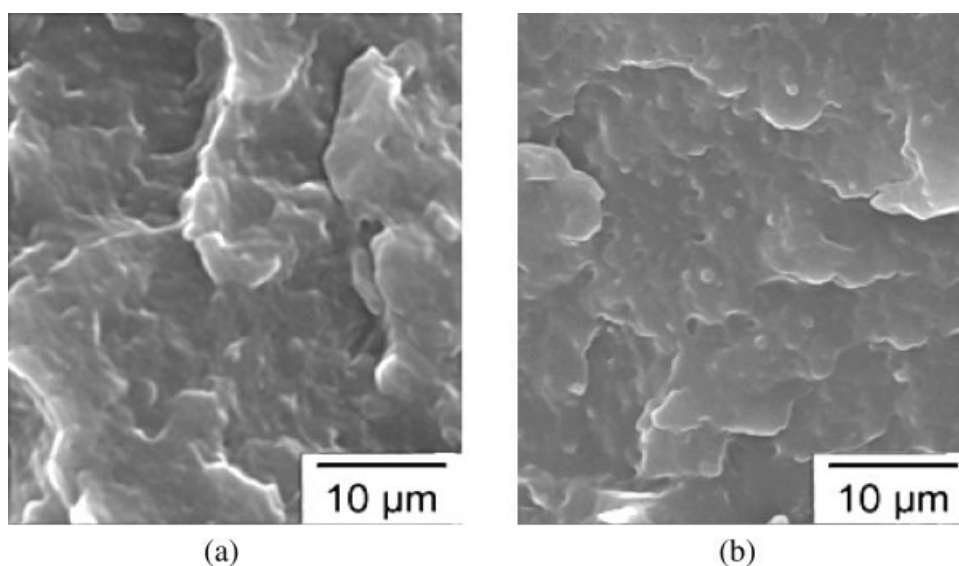


**Figure 2** SEM micrographs of the compatibilized blends: (a) PP/PA6/PPgMA (86.7/10/3.3), (b) PP/PA6/PPgMA (73.3/20/6.7).

improvement of interfacial adhesion between the PA6 particles and the matrix PP, as a consequence of the ability of the in situ formed copolymer PP-g-PA6 to reduce the interfacial tension between the dispersed phase PA6 and matrix PP suppressing the particle coalescence.<sup>4</sup> Analogous results have been showed by J. Roeder et al.<sup>3</sup> using the some compatibilizer to compatibilize blend of both virgin PP and PA6.

### Thermal properties

DSC results of the binary and ternary blends are summarized in Table I and Figure 3 displays an example of the DSC curves of PP, binary and ternary blend at the same composition (20 wt % of PA6). The binary PP/PA6 blend exhibited two separate fusion peaks (Fig. 3) originating from the melting of the PP and PA6 phases. Cooling curves show two clearly independent PA6 and PP crystallization

peaks indicating every component in the blend crystallizes independently (Fig. 3). Clearly, when the PA6 content increase in the binary blends (Table I), the heats of fusion and crystallization of the PP matrix decrease whereas, those of the dispersed PA6 phase increase. This is typical of immiscible blends. The crystallization temperature of the matrix PP alone was 112.6°C, while the corresponding temperature in the PP/PA6 blend was around 120°C in all composition. This was expected since the solidified PA6 phase enhanced nucleation in the PP phase.<sup>16</sup>

With addition of PPgMA as compatibilizer, the crystallization temperature of the PP phase was further (1–2°C) higher than the uncompatibilized blend (Table I). Since, the particle size of the dispersed PA6 phase was then smaller there was more surface area available for nucleation at the interface.<sup>17</sup> On the other hand,  $T_{c(\text{PA6})}$  are about (1–2°C) lower, an indication of slower nucleation rate,<sup>16</sup> Consequently, the

**TABLE I**  
DSC Characteristics of PP/PA6 Blends

Blend	Weight (%)	Second heating				Cooling					
		$T_f(\text{PP})$ (°C)	$T_f(\text{PA6})$ (°C)	$\Delta H_f(\text{PP})$ (J/g)	$\Delta H_f(\text{PA6})$ (J/g)	$T_c(\text{PP})$ (°C)	$T_c(\text{PA6})$ (°C)	$\Delta H_c(\text{PP})$ (J/g)	$\Delta H_c(\text{PA6})$ (J/g)	$\chi_c(\text{PP})$ (%)	$\chi_c(\text{PA6})$ (%)
PP	100/0	163.3	–	87.92	–	112.6	–	85.58	–	42.07	–
PP/PA6	95/5	162.3	219.7	83.4	1.25	120	195	82.86	1.45	39.90	0.54
	90/10	163.2	219.8	81.64	2.879	120.4	195.7	82.7	2.604	39.06	1.25
	85/15	162.95	219.8	75.41	3.57	120.6	195.5	78.26	3.66	36.08	1.55
	80/20	162.5	220	68.3	4.502	120	196.8	70.42	4.85	32.68	1.96
PP/PA6/ PPgMA	93.3/5/1.7	162.9	219.6	81	1.007	121	194.6	81.19	0.8	38.76	0.44
	86.7/10/3.3	162.5	219.4	78.92	2.025	121.2	192.6	81.13	1.857	37.76	0.88
	80/15/5	162.9	219.2	66.86	3.54	122	193.9	67.14	3.58	31.99	1.54
	73.3/20/6.7	162.5	219	60.18	4.01	122.2	194.9	65.27	4.54	28.79	1.74

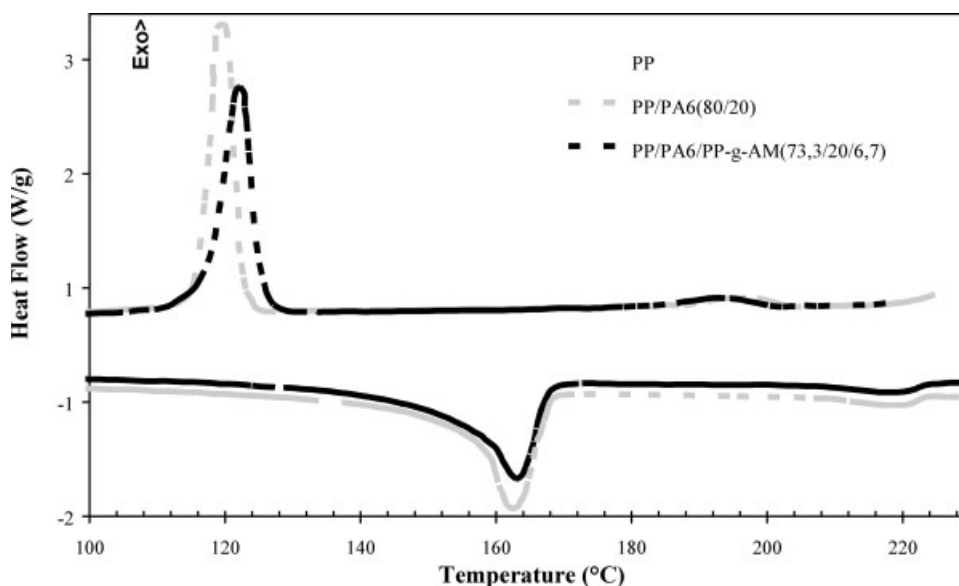


Figure 3 DSC curves of PP, PP/PA6 and PP/PA/PPgMA blend at the composition 20 wt % PA6.

presence of in situ formed PPgMA-co-PA6 copolymer tends to interfere with the PA6 crystallization.<sup>18,19</sup>

We noticed no change in the melting temperature of two phases in the uncompatibilized and in the compatibilized blends. However, crystallinity of the two components in the compatibilized blends are lower than those of uncompatibilized blend. Moreover, the copolymer molecules situated at the interface (PP-g-PA6) are able to prohibit the crystal formation according to Duvall et al.<sup>20</sup> and Paul and coworkers.<sup>21</sup>

#### Dynamic mechanical properties

The curves in Figure 4, obtained by dynamic mechanical thermal analysis, show the variation of loss modulus for PP and for the blends as a function of

temperature at various PA6 contents. Two distinct transition temperatures are recorded for PP and all the blends, one at about 6°C that corresponds to the  $\beta_{PP}$ -transition, and the other at about 52°C representing the  $\beta_{PA6}$ -relaxation and is also partially due to a secondary transition characteristic of PP ( $\alpha_{PP}$ -transition).<sup>22</sup> With increasing PA6 content in PP/PA6 blends,  $E''$  curves showed amplification in magnitude of the peak intensity for the  $\beta_{PA6}$ -relaxation. According to Murayama,<sup>23</sup> in the polymers, the intensity of each peak is a characteristic of the relative concentration of the components. In addition, the change of the  $T_g$  of PP in the blends is unnoticed however, for the dispersed PA6 phase, the glass temperature shifts to higher temperature, the  $T_g$  of PA6 in the blend increases with the composition (5–20 wt %

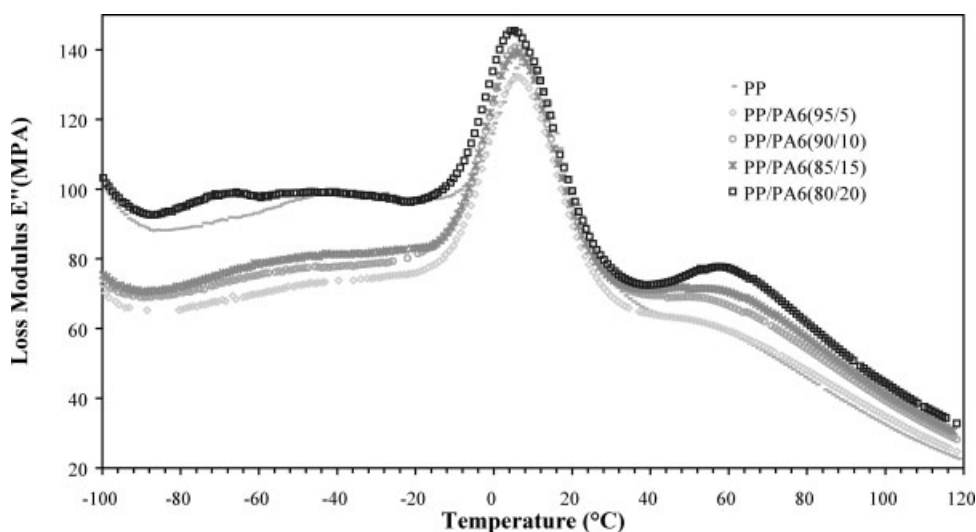
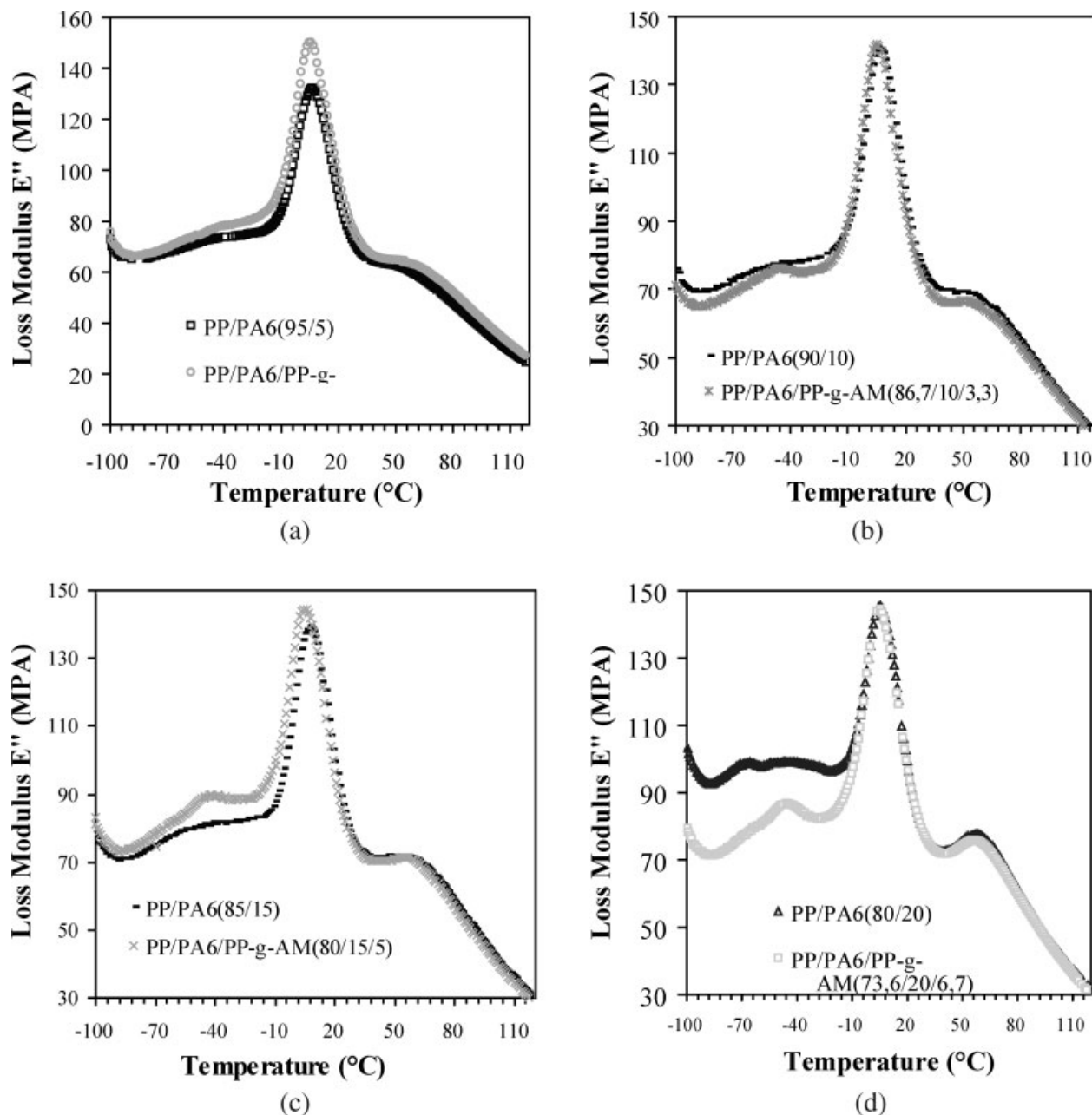


Figure 4 Loss modulus curves of noncompatibilized blends PP/PA6 (95/5, 90/10, 85/15, 80/20).



**Figure 5** Loss modulus curves of noncompatibilized and compatibilized blends for the composition: 5, 10, 15, and 20 wt % of PA6.

of PA6) from 47 to 57.6°C (Fig. 4). Consequently, this phenomenon is possibly related to the increase in the rate of crystallinity, which reduces the mobility of the amorphous polymer molecules of PA6. These results indicate that there is no evidence of adhesion between the two phases in agreement with the morphological study.

When the copolymer PPgMA are added (Fig. 5), the compatibilized blend shows unexpected behaviour. However, with the two  $E''$  maxima corresponding to the glass transitions of PP (6°C) and PA6 (52°C), an additional transition at temperatures

between  $-60$  and  $-30$ °C can be detected in all the composition and their intensity increases with the PPgMA content. Eklind et al. have reported that a small addition of PS-*g*-EO to a PPO/PMMA 30/70 blend results in a new transition at 60–100°C, with a position depending on the amount of PS-*g*-EO added.<sup>24–26</sup> This additional transition was shown to originate from the change in the relative modulus of the constituents in the interphase. So, it was reasonably concluded that the additional micromechanical transition observed in the  $E''$  curves (Fig. 5) originates from the relaxation of the amorphous chains of

**TABLE II**  
Tensile Properties of PP/PA6 Blends at a Speed of 5 mm/min

Blend	Weight (%)	Young's modulus (MPa)	Yield stress (MPa)	Elongation at break (%)
PP	100	532 ± 10	27.7 ± 0.5	861 ± 17
PP/PA6	95/5	534 ± 13	28.6 ± 0.4	746 ± 20
	90/10	552 ± 14	29.1 ± 0.2	437 ± 13
	85/15	558 ± 15	29.6 ± 0.5	400 ± 17
	80/20	534 ± 14	28.27 ± 0.5	41 ± 15
PP/PA6/PPgMA	93.3/5/1.7	546 ± 12	29.19 ± 0.6	791 ± 21
	86.7/10/3.3	584 ± 11	30 ± 0.7	465 ± 19
	80/15/5	587 ± 13	30.1 ± 0.8	431 ± 22
	73.3/20/6.7	570 ± 12	29.43 ± 0.6	57 ± 10

the copolymer PP-g-PA6 that formed the interphase in the ternary blends PP/PA6/PPgMA, with its own characteristic properties. The position and the temperature of the micromechanical transition depend, respectively, on the volume fraction and the Poisson ratio of the interphase.<sup>26</sup>

#### Mechanical properties under tension:

The mechanical properties of the pure polymers PP and their blends are summarised in Table II and for comparison Figure 6 shows nominal stress–strain curves of PP and PP/PA6 blend for 10 wt % PA6.

During tensile tests, PP and the blends with compositions of PA6 ≤ 15 wt % were considerably deformed before breaking in the condition used for the tests. However, the PP/PA6 (80/20) blend displays a small deformation at break (≈ 41%) (Table II), its tensile properties at weak deformation are also lower than the other blends. The addition of PA6 to

PP results in a small increase of the tensile modulus and yield stress as a result of the reinforcing effect of the higher modulus and higher yield stress of PA6.<sup>15</sup> However, the reinforcing effect of the PA6 dispersed phase is highly inefficient, owing to a combination of poor interfacial bonding between these immiscible polymers and the coarse dispersed phase morphology resulting from coalescence (Fig. 1). Thus, the ductility of the blend decreased with the increasing of PA6 content compared to the PP reference (Fig. 6).

Auditioning the compatibilizer PPgMA to the PP/PA6 blend resulted in improvement of their tensile properties (Table II), it can be seen in Figure 6 that the ductility of the compatibilized blend increase compared to the uncompatibilized blend at the same composition indicating that the interphase between PP and PA6 adheres strongly to both phases and tolerate the stress transfer between the matrix and the dispersed phase. The Young's modulus, and the yield stress are also slightly amplified (Table II). The improvement of tensile properties can be attributed to the significant change of their morphologies (Fig. 2) and the improved interfacial adhesion among both phases.<sup>16</sup>

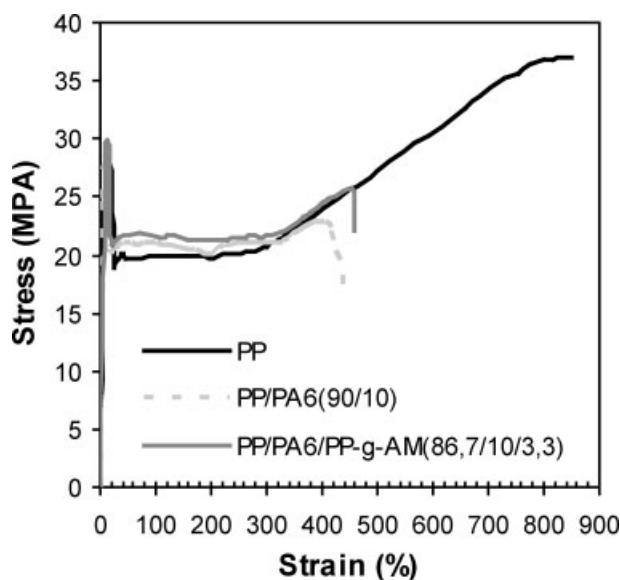


**Figure 6** Stress–strain curves of PP, PP/PA6, and PP/PA6/PPgMA blend at the composition 10 wt % PA6 at a speed of 5 mm/min.

#### CONCLUSIONS

Blending of polypropylene with PA6 industrial waste is an important way of valorization. Although, binary PP/PA6 blend exhibited a coarse morphology and a lower adhesion between both phases results in the decrease of ductility of materials with the decrease of PA6 content. Addition of PA6 waste leads to an increase of Young's modulus and yield stress. In the compatibilized PP/PA6/PPgMA blend, SEM images indicate that the copolymer PP-g-PA6 formed in situ at the interface induces a finer dispersion of PA6 into PP matrix, this copolymer is identified by DMA analysis with the additional transition observed in the  $E''$  curves, which was shown to originate from the relaxation of their amorphous chains.

Besides, the interfacial adhesion is expected to be increased and results in lower crystallinity and in better tensile properties. From an applicative point of view, 20 wt % PA6 can be blended with PP without affecting Young's modulus and yield Stress but decreasing elongation at break. The compatibilizer leads to smaller diameters of the dispersed phase and should enhance impact properties.

## References

1. Sacchi, A.; Landro, L. Di.; Pegoraro, M.; Severini, F. *Eur Polym J* 2004, 40, 1705.
2. Zhong-Zhen, Y.; Ming-Shu, Y.; Shao-Cong, D.; Yiu-Wing, M. *J Appl Polym Sci* 2004, 93, 1462.
3. Roeder, J.; Oliveira, R. V. B.; Gonçalves, M. C.; Soldi, V.; Pires, A. T. N. *Polym Test* 2002, 21, 815.
4. Li, Z.; Xiaomin, Z.; Shigeru, T.; Norihiro, I. *Mater Lett* 2001, 48, 81.
5. Nishio, T.; Yokoi, T.; Nomura, T.; Ueno, K.; Akagawa, T.; Sakai, I. (to Toyota Jidosha). U.S. Pat. 4, 988 (1991).
6. Mashita, K.; Fujii, T.; Oomae, T. (to Sumitomo Chemical). U.S. Pat. 4, 780 (1988).
7. Ide, F.; Hasegawa, A. *J Appl Polym Sci* 1974, 18, 963.
8. Ikkala, O. T.; Holsti-Miettinen, M. R.; Seppeala, J. *J Appl Polym Sci* 1993, 49, 1165.
9. Holsti-Miettinen, R.; Seppeala, J.; Ikkala, O. *Polym Eng Sci* 1992, 32, 868.
10. Reosch, J.; Meulhaupt, R. *Prepr ADSC Div Polym Mater: Sci Technol* 1994, 70, 193.
11. Folkes, M. J.; Hopes, P. S. *Polymer Blends and Alloys*; Blackie Academic: London, 1993; Vol. 1, p 60.
12. Vocke, C.; Anttila, U.; Heino, M.; Hietaoja, P.; Sepala, J. *J Appl Polym Sci* 1998, 70, 1923.
13. Ralua, N. D.; Mihai, B.; Cornlia, V. *Polym Degrad Stab* 2003, 80, 551.
14. Khanna, Y. P.; Kuhn, W. P. *J Sci Part B: Polym Phys* 1997, 35, 2219.
15. Wilkinson, A. N.; Laugel, L.; Clemens, M. L.; Harding, V. M.; Marin, M. *Polymer* 1999, 40, 4972.
16. Tseng, F.-P.; Lin, J.-J.; Tseng, C.-R.; Chang, F.-C. *Polymer* 2001, 42, 719.
17. Hippi, U. *Polymer Technology Publication Series No. 27*; Espoo, 2005.
18. Beltrame, P. L.; Castelli, A.; Canauz, M.; Canetti, M.; Seves, A. *Macromol Chem Phys* 1995, 196, 2751.
19. Lee, J. D.; Yang, S. M. *Polym Eng Sci* 1995, 35, 1821.
20. Duvall, J.; Sellitti, C.; Myers, C.; Hiltner, A.; Bear, E. *J Appl Polym Sci* 1994, 52, 207.
21. Gonzalez-Montiel, A.; Keskkula, H.; Paul, D. R. *J Polym Sci Part B: Polym Phys* 1995, 33, 1751.
22. Liang, Z.; Williams, H. L. *J Appl Polym Sci* 1992, 44, 699.
23. Murayama, T. *Mater Sci Monogr* 1978, 1, 90.
24. Eklind, H.; Schantz, S.; Maurer, F. H. J.; Jannasch, P.; Wessln, B. *Macromolecules* 1996, 29, 984.
25. Eklind, H.; Maurer, F. H. J. *Polymer* 1996, 37, 2641.
26. Eklind, H.; Maurer, F. H. J. *J Polym Sci Part B: Polym Phys* 1996, 34, 1569.